*Article*

# Design and Analysis of the Slider Shear Test System Using Nested GR&R Measurement System

**Santi Pumkrachang[1], Krisada Asawarungsaengkul[2,*], and Parames Chutima[3]**

1 Department of Industrial Engineering, Faculty of Engineering, King Mongkut's University of Technology North Bangkok, Bangkok 10800, Thailand
2 Operations Research and Engineering Management Research Center, Department of Industrial Engineering, Faculty of Engineering, King Mongkut's University of Technology North Bangkok, Bangkok 10800, Thailand
3 Department of Industrial Engineering, Faculty of Engineering, Chulalongkorn University, Bangkok 10300, Thailand

*E-mail: krisada.a@eng.kmutnb.ac.th (Corresponding author)

**Abstract.** The shear strength of the adhesive bonding between slider and suspension is a vital characteristic for head gimbal assembly. The current shear test method has shown improper failure modes; therefore, a new system has been designed to improve the slider shear test. Six sigma framework was applied to redesign the slider shear test system. The finite element method confirms that new design concept is acceptable because it can yield the correct failure mode of shear test. Next, the measurement errors of the new shear test system are assessed using nested gage repeatability and reproducibility (NGR&R). NGR&R of new shear test system is less than 10% which is an adequate gage. Then, the results of simulation also confirm that decreasing of measurement error can significantly reduce the over reject rate. In conclusion, new shear test system can be effectively used to reflect the real product quality and to obtain more accurate process capability resulting from the correct failure mode of testing.

**Keywords:** Epoxy adhesive, design of slider shear test system, finite element method, measurement system analysis, process capability.

## 1. Introduction

A hard disk drive is a magnetic recording component of a computer system that stores data and information into the magnetic platter through the magnetic read/write heads. The head gimbal assembly (HGA) acts as the reading and writing component that is flying on the disk media while spinning at the high rotation speed such as 7,200, 10,000, 12,000 or 15,000 RPM etc. The HGA is an assembled component composed of a "slider," which is used for reading or writing data and "suspension," which is the body of the HGA. A suspension consists of three components including the base plate, the load beam, and the flexure which are welded to be an assembly part. The flexure is an electrical circuit that connects to the slider and can have many layers. The load beam is the base of flexure while the base plate is the part that will be mounted to the actuator arm of the head stack assembly (HSA).

For hard disk drive (HDD) manufacturer, the quality and reliability of product is important to the customer because the poor product quality greatly impacts to the data loss of the data storage systems. The attachment process of a slider to a suspension uses epoxy adhesive for creating bonding connections between the slider and the suspension. The slider is placed on the bonding pad of the flexure. Since HGA which flies at a height of 10-20 nanometers over the disk media during high spindle speed of media disk may hit to the disk; the shear strength of the adhesion bonding between the slider and suspension after the curing process is a vital quality check. The measurement of the key quality characteristics is typically performed to reflect the capability of the manufacturing process. Therefore, this paper focuses on evaluating, redesigning, and improving the shear test procedure so that the suitable shear test method for the adhesive bonding will be obtained.

The current shear test system cannot deliver the accurate and precise shear test result because of the incorrect failure mode of testing. It was found that there is no international standard for the shear test of the adhesive joint of the slider in HGA. To receive an accurate measurement with proper adhesive shear test results, an appropriate test equipment is proposed. The study of the adhesive strength for the various types of epoxy adhesives, types of materials, joint types, testing methods, testing conditions, mechanical properties, the structure of the adhesive, failure modes, and experiment procedure can be found in some papers such as [1], [2], [3], [4], [5], [6], [7], [8], [9], [10], and [11], etc. Based on these papers, it is seen that the bonding area or joint area is larger than the bonding area of the HGA product. The size of the specimens used in the shear test of those papers were also much bigger than the size of the HGA. Therefore, the design of the test fixture for the HGA product was done with some constraints because the component of the HGA is very thin and small. The clamping area of the fixture on the HGA is very small and limited as well.

The single lap shear (SLT) test, which is a typical method for evaluating the strength of adhesive and other alloy joints, was discussed in [2], [4], [5], [6], [7], [8], [10], [11], [12], etc. The LST is typically performed using the universal tensile test. Both sides of the specimen are griped and then shear force is applied to measure the force and displacement. The single lap shear test standards such as [13], [14], and [15], were used in [4], [8], [10],.[12] A review of the prediction of several types of adhesive joints was also presented in [9]. The purposes of the SLT in these papers were to investigate the shear strength, the failure mode, and the structure of the bonded joint.

The shear test for the adhesive joint of slider has been done on the product level as the destructive testing. This shear test is the part of process control of HGA. Some of the papers performed the shear strength at product level such as [1], [3], [16], [17], [18] and [19], etc. A solder ball shear test was proposed by [16]. Pb-free and SnPb solder were tested with various shear rates in order to observe the shear force. [1] presented the shear strength of the die attachment by Ag-epoxy electrical conductive adhesive (Ag-ECA) which was tested under many treatments including the heating/cooling process, adhesive thickness, and plating condition. The die shear strength of the die attach film tested with various temperatures was done by [3]. The shear strength of SAC305 and the sintered nanosilver joint for the die attachment in the IC package were studied in [17] and [18]. The experimental investigation and finite element study of a button shear test to measure shear force and displacement was proposed by [19]. A standard of the die shear test for semiconductor package has been defined in [20]. This shear test method can be modified to be used for the adhesive shear test for the slider bonding process.

The fixture is normally required in the adhesive shear test. To appropriately hold the HGA during the shear test, the fixture must be designed by considering the shape of suspension. The fixture and equipment design for the joint shear test have been presented in some papers as in [21], [22], [23], etc. [21] focused on the design of shear testing equipment that can be used for multi-purpose specimens. An adhesive shear jig for the semiconductor package was designed by [22] to measure the shear strength. The design and assessment of the adhesive fixture for measuring the strength and the effect of different film thickness, curing time and pre-cleaning on strength repeatability was performed by [23].

The measurement error is a concern issue for the slider bonding process. The nested gage repeatability and reproducibility was employed to assess the measurement error in this study because the adhesive shear test is a destructive test. Some of the literature on the application of the GR&R to assess the measurement system can be found in [24], [25], [26], [27], [28], etc. The NGR&R for the shear test for spot welding was done by [26]. The NGR&R was applied in the measurement of wind speed [27] and the measurement of angle of repose [28].

Based on the current problem and information in the introduction, this paper proposes the design of the new tester equipment and the evaluation of the measurement error to achieve the suitable failure mode and to obtain the

acceptable precision of the measurement system. The proposed slider shear test system will yield more reliable process control for the HGA assembly process. Thus, the main procedures of this paper include: the experiment investigation of current slider shear test system, design and fabricate of the shear test method, the measurement system analysis, and the effect of measurement error to the over reject rate. The proper analytical methods such as the finite element method, the statistical analysis, and the simulation technique will be utilized to assist the design and evaluation of the proposed slider shear test system.

## 2. Material and Methodology

The overall framework of this paper is based on the six sigma methodology as in Fig. 1. Define measure, analyze, design, and verify are main procedures to achieve the objective of this work. In define phase, the problem statement for the current shear test method should be clearly defined. The observation on the failure mode obtained from the current slider shear test system was firstly conducted to identify need of improvement for this measurement system.
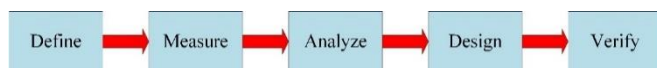


Fig. 1. The six sigma methodology for improving the slider shear test system.

### 2.1. Mathematics

The epoxy adhesive, slider, and flexure were the main materials in this study. The adhesive's chemical composition is presented in Table 1. The flexure in the HGA has three layers, which were made from stainless steel, copper, and polyimide (Pi). The slider was made of aluminum titanium carbine (Al-TiC). The mechanical properties of the HGA components are needed for the FEM are given in Table 2. The finite element method (FEM) was employed in order to analyze the stress and deformation of the HGA after applying the shear force. Some papers have employed the FEM to perform the analysis on the strength of the adhesive joint as in [6], [8], [10], [19], [22], and [23]. [6] used the FEM to evaluate the effect of the slightly oversized shear tool to the joint shear strength. [19] performed the FEM in order to observe the displacement on the button when the substrate thickness was varied.

Table 1. Chemical composition of the adhesive used in this research.

| Element | 3,4-Epoxycyclohexylmethyl -3,4-epoxycyclohexane carboxylate (EEC) | Resin Copolymers | Amorphous fumed silica | Butyrolactone |
|---|---|---|---|---|
| % Weight | 35% | 50% | 10% | 5% |

Table 2. Mechanical properties of HGA components.

| Material | Stainless steel | Copper | Polyamide | Adhesive |
|---|---|---|---|---|
| Yield Strength (MPa) | 1,150 | 70 | 286 | 5.31 |
| Tensile Strength (MPa) | 1,186 | 314 | 286 | 5.31 |
| Poison's ratio | 0.31 | 0.34 | 0.33 | 0.24 |
| Young's modulus (MPa) | 193,000 | 124,000 | 5,860 | 4.40 |

### 2.2. The Investigation on the Problem of the Current Slider Shear Test System

The investigation on the slider shear test system was conducted to define problem of the current measurement system. The current slider shear test system in the HGA process is illustrated in Fig. 2. The schematic detail of the current shear test is shown in Fig. 3. The concept of this method is to use a gripper for holding the slider on both sides, and then to insert the hook, which is made of stainless steel, in the hole of the base plate of the suspension. After that, the suspension is moved in the upward direction by a constant velocity of 0.25 mm/s. The maximum adhesive shear force is measured by using force gauge and displayed after completing the measurement for each HGA.

The bonding pad and the slider after matting onto the bonding pad are depicted in Fig. 4(a). Typically, the suitable failure mode of the shear test must occur at the adhesive bond line as shown in Fig. 4(b). After the shear test, the results of shear test sometimes show a flexure collapse. This inappropriate failure modes as seen in Fig. 4(c) and Fig. 4(d) indicate that the maximum shear force may not directly come from the adhesive bond line between the slider and suspension pad. This investigation reveals that the slider shear test system faces the low accuracy and precision problem. To solve this problem, the schematic of the current slider shear test system must

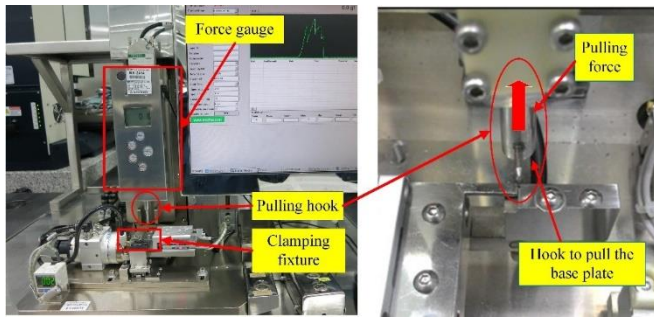be investigated. Then, new slider shear test system was proposed to avoid the incorrect failure modes.



Fig. 2. The current slider shear test system for the slider bonding process of HGA.

## 2.3. Measurement System Analysis for the Current Slider Shear Test System

The assessment of the measurement system is required for the measure phase of six sigma. In terms of the precision, the measurement system error for the current slider shear test system must be assessed using nested gage repeatability and reproducibility. The analysis of variance was mainly used to estimate the measurement error as in [28], [25], [26], [27], [24], etc.
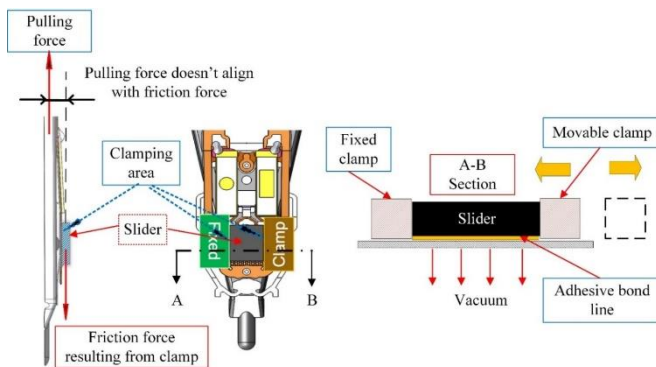


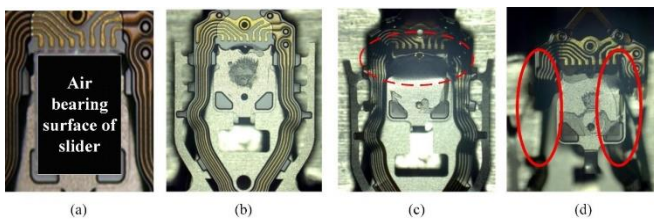Fig. 3. A schematic of the current adhesive shear test used in the slider bonding process.



Fig. 4. (a) HGA before shear test; (b) proper failure mode required; (c) incorrect failure mode occurred at the suspension pad; (d) incorrect failure mode occurred at the outrigger flexure.

The measurement systems analysis is crucial to determine the measurement error of the tester or gage. Gage repeatability and reproducibility (GR&R) studies examine the variation of the process affected by measurement variation. Repeatability is the measurement

error due to gage by assign each operator performs the repeat measurement on the same part on that specific tester. Reproducibility is the measurement variability resulting from operators that measure the same part using the same tester. In destructive testing, the measured sample is damaged after the measurement process. Nested GR&R study is used for analyzing the measurement error of gage for the destructive test. Then, NGR&R is also used to evaluate the new tester and to verify that the new slider shear test system has high precision in assessing the shear strength of the adhesive bonding.

Analysis of variance was utilized to estimate the variance components (VarComp) for each source of measurement variation. [29] reported that ANOVA method is the suitable method to assess the GR&R. The formula for the sum of squares (SS), which is the amount of variability in the data due to different sources, can be found in [27] and [30]. There is no interaction between part and operator because not every level of part appears with every level of operator, see [30]. Mean squares or variance components in NGR&R study consist of repeatability, reproducibility, part-to-part (or process), total gage R&R, and total variation.

The variables in ANOVA shown in Table 4 can be defined by the following information: $y_{ijk}$ is an observation; $\bar{y}_{.j.}$ is the mean for operator $j$; $\bar{y}_{...}$ is the grand mean; $\bar{y}_{ij.}$ is the mean for part $i$ within operator $j$; $a$ = number of parts, $b$ = number of operators, $n$ = number of replicates

The linear statistical model of ANOVA for NGR&R can be defined as in Eq. (1), see [27] and [31].

$$Y_{ijk} = \mu + \tau_j + \beta(\tau)_{i(j)} + \varepsilon_{ijk} \quad \begin{cases} i=1,...,a \\ j=1,...,b \\ k=1,...,n \end{cases} \quad (1)$$

where $Y_{ijk}$ is the variable of measured value; $\mu$ is the average of measured value; $\tau_j$, $\beta(\tau)_{i(j)}$, $\varepsilon_{ijk}$ are the effect of operators, parts nested with operators, and the random error, respectively. All effects and the random error in Eq. (1) are normally distributed with a mean of zero.

All variance components ($\sigma^2$) for NGR&R can be computed according to Eq. (2) to Eq. (6), see [27] and [30].

$$\sigma^2_{Repeatability} = MS_{Repeatability} \quad (2)$$

$$\sigma^2_{Repeatability} = \frac{MS_{Operator} - MS_{Part(Operator)}}{an} \quad (3)$$

$$\sigma^2_{Part-to-Part} = \frac{MS_{Part(Operator)} - MS_{Repeatability}}{n} \quad (4)$$

$$\sigma^2_{Total\ Gage\ R\&R} = \sigma^2_{Repeatability} + \sigma^2_{Reproducibility} \quad (5)$$

$$\sigma^2_{Total\ Variation} = \sigma^2_{Total\ Gage\ R\&R} + \sigma^2_{Part-to-Part} \quad (6)$$

Design of experiment (DOE) was utilized to evaluate the precision of the current slider shear test system using the NGR&R study. The result of the NGR&R study will enable us to know the source of the variation due to the gage and operator-to-operator.

Table 3. The analysis of variance for NGR&R.

| Source | Degree of freedom | Sum of squares (SS) | Mean squares (MS) | F |
|---|---|---|---|---|
| Operator | $b-1$ | $SS_{Operator} = an\sum_{j=1}^{b}(\bar{y}_{.j.}-\bar{y}...)^2$ | $\dfrac{SS_{Operator}}{(b-1)}$ | $\dfrac{MS_{Operator}}{MS_{Part(operator)}}$ |
| Part (Operator) | $b(a-1)$ | $SS_{Part(Operator)} = n\sum_{i=1}^{a}\sum_{j=1}^{b}\left(\bar{y}_{ij.}-\bar{y}...\right)^2$ | $\dfrac{SS_{Part(operator)}}{b(a-1)}$ | $\dfrac{MS_{Part(operator)}}{MS_{Repeatability}}$ |
| Repeatability | $ab(n-1)$ | $SS_{Repeatability} = \sum_{i=1}^{a}\sum_{j=1}^{b}\sum_{k=1}^{n}\left(y_{ijk}-\bar{y}...\right)^2$ | $\dfrac{SS_{Repeatability}}{ab(n-1)}$ | |
| Total | $abn-1$ | $SS_{Total} = SS_{Operator} + SS_{Part(Operator)}$ $+SS_{Repeatability}$ | | |

The design of experiment provides the plan to collect data for the MSA. Three operators ($b = 3$) were selected to be appraisers. There were 10 batches of HGA ($a = 10$), and three replicates (n = 3) of each batch were tested by three operators. The range of the adhesive dot size was from 84.6 µm to 128 µm. The total runs of 90 for DOE were tested randomly. The response variable of this experiment is shear force. The %Contribution of variance component (VarComp) and %NGR&R can be used as the indicator to assess whether the gage is acceptable or not. Both indicators can be computed as in Eq. (7) and (8):

$$\% \, Contribution = \frac{\sigma^2_{Total \, NGR\&R}}{\sigma^2_{Total \, Variation}} \times 100\% \qquad (7)$$

$$\% \, GR\&R = \frac{\sigma_{Total \, NGR\&R}}{\sigma_{Total \, Variation}} \times 100\% \qquad (8)$$

Based on the recommendation from the Automotive Industry Action Group [31], %GR&R is an indicator used for making the decision in accepting a gage. The general guidelines of the AIAG for measurement system acceptability in terms of %GR&R are as follows: (1) under 10% is acceptable, (2) 10% to 30% is acceptable for some applications, and (3) over 30% is unacceptable.

The experiment data for the nested GR&R of the current shear test system is shown in Table A.1. According to Table 4, %NGR&R is 57.15% which is unacceptable because it is greater than 30%. A high %NGR&R indicates that the current method generates high measurement error, and this can affect the judgment on product quality. Thus, the current measurement system must be improved to reduce the repeatability.

The graphical plot of Xbar and R chart are provided in Fig. 5. The Xbar chart indicates that the distinguishing ability of the gage is low. The R Chart does not show any out-of-control points which means that the variance is stable. The distinguishing ability between parts of the gage can be observed via the number of distinct categories (NDC), see [31]. An NDC greater than or equal to five is recommended by [31]. The NDC of the current slider shear test system equals 2; thus, this measurement system lacks the ability to distinguish the parts.

Table 4. %Contribution of VarComp and %NGR&R for the current slider shear test system.

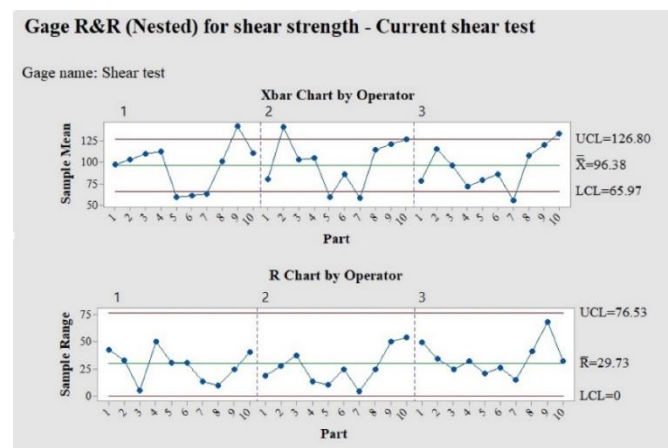| Source | VarComp ($\sigma^2$) | %Contribution (of VarComp) | Standard Deviation($\sigma$) | %NGR&R |
|---|---|---|---|---|
| Total Gage R&R | 296.524 | 32.66 | 17.2199 | 57.15 |
| Repeatability | 296.524 | 32.66 | 17.2199 | 57.15 |
| Reproducibility | 0.00 | 0.00 | 0.00 | 0.00 |
| Part-To-Part | 611.300 | 67.34 | 24.7245 | 82.06 |
| Total Variation | 907.824 | 100.00 | 30.1301 | 100.00 |



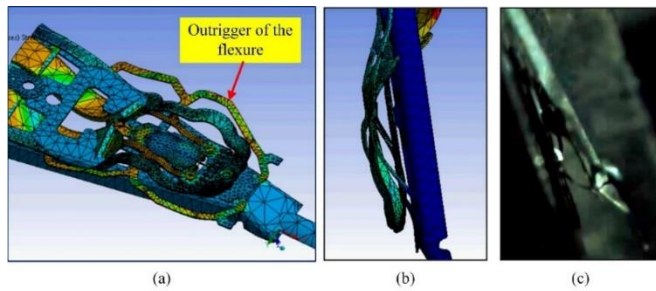Fig. 5. Xbar and R chart of NGR&R study for the current shear test method.

Fig. 6. Deformation on the HGA under the current test method; (a) deformation from FEM (top view); (b) deformation from FEM (side view); (c) deformation from the high-speed camera.

## 2.4. Validation of the Simulation Model for the Current Slider Shear Test System

The analyze phase intends to determine the root causes of the inappropriate failure modes from the current test equipment. In this study, the finite element analysis of Ansys Workbench Version 15.0 was the tool for analyzing the deformation behaviors and mechanical stress. The FEM tried to simulate the schematic of the current testing conditions shown in Fig. 3. The slider was moving in the vertical direction at the speed of 0.25 mm/s. The components exhibit a nonhomogeneous stress distribution. With the general three-dimensional axis-symmetric, a static model was developed to calculate the distribution of stress and the displacement of the suspension when the current shear test method was used. The results of FEM are illustrated in Fig. 6(a) and Fig. 6(b).

A high-speed microscope camera (Keyence VW-9000) is utilized to capture this very tiny object to validate the shear test behavior during the test operation. The high-speed microscope camera at the magnification of 50x, with a frame rate of 1000 fps and shutter speed of 1/3000 was setup. The results from high-speed camera showed that high deformation occurs at both sides of the flexure, as illustrated in Fig. 6(c). It was found that a shearing position often occurred at the outrigger of flexure, which was sometimes weaker than the adhesive bond line. This failure mode of the sheared sample on the current fixture did not seem to be the right mode, see Fig. 4(c), and 4(d). The FEM results and experiments observed from the high-speed camera were in good agreement. Therefore, it could be implied that the FEM was valid and could be used to validate the new shear test method. This observation indicated that the current slider shear test system is inaccurate. The observed shear strength value then became the strength of the flexure material rather than the strength of the adhesive bond line. Thus, high variation in the measured shear force was noticed.

## 2.5. Design Concept of the New Slider Shear Test System

In design phase, a new design concept was proposed to solve the inappropriate failure during shear test. Since three thin layers of the suspension were assembled using

laser spot welding, new shear test method tries to avoid the flexure movement. Therefore, the flexure and load beam needed to be firmly clamped before applying shear force to the adhesive joint of slider. The major objective of new shear equipment was to increase the accuracy and precision of this shear test. The concept of the shear test method is depicted in Fig. 7(a) and 7(b). The shear force was directly applied to the slider, which is similar to the standard of die shear test defined by JEDEC standard [20], but the fixture for holding and clamping must be designed to fit the configuration of the HGA. Papers on joint shear tests using the shear tool to apply force to the component was done by [18], [19], [32].

Regarding the new concept of the shear test, the degree of freedom could be reduced to 1 degree by fixing the components at the flexure and load beam areas, as shown in Fig. 7(b) and Fig. 7(c). In this way, the new design mechanism focused on the design of the fixture in order to firmly hold the flexure and load beam of the suspension on the fixture. The outrigger must be appropriately placed in the supporting area and clamping area on the outrigger must be large enough to match the clamping pressure.

The FEM was utilized to confirm the displacement of the flexure after the shear test with the new clamping fixture. The flexure is fixed by applying the pressure of 0.5 MPa (5 bars) onto the clamping symmetrically as shown in Fig. 7(c). The shear force of 200 gf, which is the expected maximum shear force of the new platform of the HGA, was applied to the slider. The total deformation of 165.72 microns was observed by the FEM as seen in Fig. 7(d). The movement of flexure is much smaller than that of the current test method. This comparison indicates that the new concept of shear test method can improve the accuracy of the shear test because of the correct failure mode. The experiment on the actual equipment is presented in the next section.

## 3. Experiments and Results

In verify phase, the new shear test must be verified to ensure that the design of new test system can be used to solve the problem of the current measurement system.

### 3.1. Validation of Failure Modes from the New Slider Shear Test System

New slider shear test system as seen in the Fig. 8(a) was used to observe the failure mode and to measure the shear strength of the adhesive joint of slider. A Mecmesin AFG analyzed the shear strength distribution of the bonding interface. This analyzer used the computerized control with a 0.001N resolution and a 5N maximum load. The shear test motor speed was carried out on a Panasonic servo motor (MUMA042P1S) connected to the gearbox (APEX dynamics Inc., model AE070), and the shear speed was 200 μm/min. After the adhesive joint was pushed out by the shear tool, the shear force – distance curve was plotted as shown in Fig. 8(b).

The operation of the slider shear test system can begin with loading the HGA onto the fixture by using tweezers, and then rotating the c-shape clamp on the top of the outrigger. Vacuum pressure will assist the load beam in staying in the pocket easily. Next, clamping force from pneumatic cylinder is applied onto the outrigger. The actual shear tools, as depicted in Fig. 8(a), begin to move and push the slider edge at a 200 μm/minute speed until the slider is sheared out at the designated location. A software was developed to display the plot of shear force and distance is displayed, see Fig. 8(b).
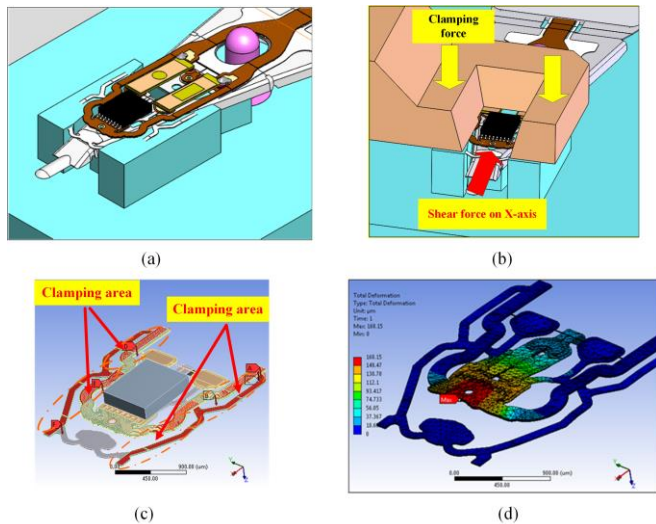


Fig. 7. (a) Pocket and guide pin to hold HGA; (b) clamping fixture design for new test equipment; (c) clamping area in the FEM; (d) the maximum deformation form FEM.
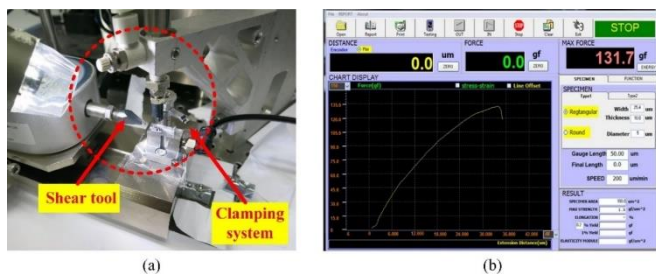


Fig. 8. (a) New slider shear test system with direct shear tool and fixture for the adhesive shear test of the HGA; (b) force (gf)-distance (micron) plot of the adhesive shear test.

Figure 9 shows the shear tool which was fabricated in order to investigate the actual failure modes. The clamp and new shear tool were designed and illustrated in Fig. 9(a) and Fig. 9(b), respectively. The preferable failure mode after shearing shown in Fig. 9(c) could be obtained by applying the shear force in front of the slider. The clamp fixture and shear tool can improve the accuracy with an excellent mechanical appearance without any damage to the flexure or load beam. The consistency of failure mode of the new shear test method can improve not only the accuracy but also the precision of the shear strength of the adhesive joint of slider.
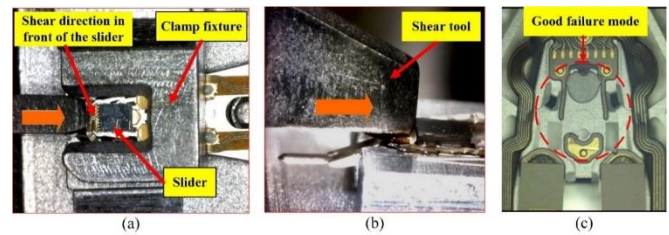


Fig. 9. (a) Clamping fixture to press the suspension; (b) shear tool of new test method; (c) preferable failure mode obtained from new test method

Table 5. % Contribution of VarComp and %NGR&R for the new slider shear test system.

| Source | VarComp ($\sigma^2$) | %Contribution (of VarComp) | Standard Deviation($\sigma$) | %NGR&R |
|---|---|---|---|---|
| Total Gage R&R | 4.35 | 0.86 | 2.0857 | 9.28 |
| Repeatability | 4.35 | 0.86 | 2.0857 | 9.28 |
| Reproducibility | 0.00 | 0.00 | 0.00 | 0.00 |
| Part-To-Part | 500.805 | 99.14 | 22.3787 | 99.57 |
| Total Variation | 505.156 | 100.00 | 22.4757 | 100.00 |
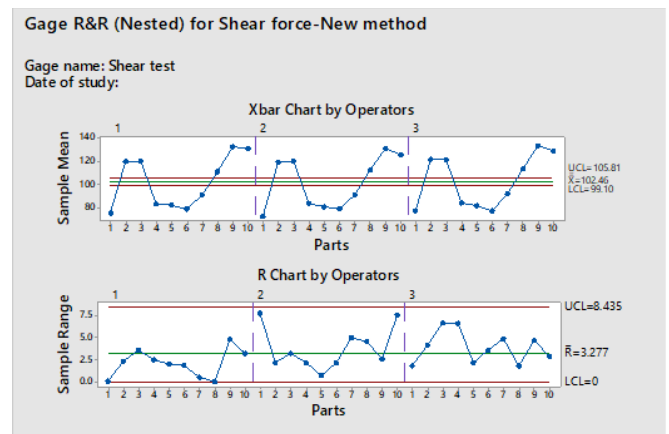


Fig. 10. Xbar and R chart for NGR&R analysis of the new shear test method.

### 3.2. Assessment of the Measurement Error for the New Slider Shear Test System

The new shear test method has already been built to reduce the measurement error. Next, another experiment was also done in order to determine the measurement error of the new slider shear test system. The experiment data for the NGR&R based on DOE plan of the new slider shear test system is also displayed in Table A.2. The NGR&R study is shown in Table 5. It is seen that the new slider shear test system contributes to a %NGR&R of 9.28%. The measurement error of this new shear tester can be considered as a good gage because the %NGR&R is less than 10%. Therefore, this new tester can be used to measure the shear force of the HGA product with high confidence. For the new tester, the R chart in Fig. 10

indicates that the variance of repeat measurement for each operator is stable. The number of distinct categories of this gage is equal to 15 which is greater than 5. Therefore, this measurement system has enough ability to distinguish the parts.

### 3.3. Effect of Measurement Error to the Observed Process Capability

The high measurement error results in inaccurately estimating the process capability. The assessment of the process capability index using sampling plan with the presence of measurement error was done in [33]. It was found that high measurement error can affect the effectiveness of statistical process control. A good review on the measurement error in statistical process control was presented in [34]. The impact of the NGR&R on the process capability index [31] could be computed using Eq. (9) as follows:

$$Cp_{Obs} = Cp_{Act} \times \sqrt{1-(NGR\&R)^2} \qquad (9)$$

where $Cp_{Obs}$ is the observed potential process capability index; $Cp_{Act}$ is the actual potential process capability index.

The difference between the observed potential process capability of the new and current shear test method ($\Delta Cp_{Obs}$) can be calculated as follows:

$$\Delta Cp_{Obs} = \frac{Cp_{Obs,New} - Cp_{Obs,current}}{Cp_{Obs,current}} = \frac{\sqrt{1-(NGR\&R_{New})^2}}{1-(NGR\&R_{Current})^2} - 1 \qquad (10)$$

where $\Delta Cp_{Obs}$ is the difference of the observed $Cp$ between the new and current shear test method.

Reducing of measurement error (%NGR&R) in the new slider shear test system can improve the accuracy in estimating $Cp$. According to Eq. (10), the observed potential process capability ($Cp$) of the new shear test method is increased by 21.28% compared to that of the current shear test method. The defective rate in the unit of part per million (PPM) can be estimated by process capability indices: $Cp$ or $Cpk$. For one-side specification limit (LSL), both $Cp$ and $Cpk$ are identical. The formula to calculate the PPM given $Cp$ or $Cpk$ can be written as in Eq. (11):

$$PPM = 1 - \Phi(Z_{LSL}) = 1 - \Phi(3Cp) = 1 - \Phi(3Cpk) \qquad (11)$$

where ZLSL is the benchmark Z statistics for LSL (lower specification limit); $\Phi(Z)$ is the cumulative distribution function of a standard normal distribution; $Cpk$ is the performance process capability index; and PPM is the defective rate in part per million. The measurement system with high measurement error will yield the high observed variation of the process.

The over reject (OR) in case of one-side specification limit resulting from the measurement system error can be calculate by Eq. (12):

$$OR = PPM_{Obs} - PPM_{Act} = \Phi(3Cp_{Act}) - \Phi\left(3Cp_{Act}\sqrt{1-(NGR\&R)^2}\right) \quad (12)$$

where PPM_Obs is the defective rate in part per million estimated by $Cp_{Obs}$; PPM_Act is the defective rate in part per million estimated by $Cp_{Act}$; $OR$ is the over rejected rate.

### 3.4. Monte Carlo Simulation to Observe the Effect of the NGR&R to the Process Capability

The monte carlo simulation is employed to validate the effect of measurement error to the misclassification problem. The process capability can be presented in the form of PPM. For the shear strength, there is only one-side specification which is the lower specification limit as the lower bound for capability index. Monte carlo simulation generates the random variable using the inverse cumulative distribution function (CDF). The inverse cumulative distribution function of the normal distribution $N(\mu, \sigma^2)$ is shown in Eq. (13).

$$x = F^{-1}(p) = \mu + \Phi^{-1}(p)\sigma \;\; ; p\epsilon(0,1) \qquad (13)$$

where x is a normal random variable or shear strength with mean $\mu$ and variance $\sigma^2$, $\Phi^{-1}(p)$ is the inverse of the cumulative distribution function for the standard normal distribution.

The sampling method of monte carlo technique uses the continuous uniform random number $U(0, 1)$ to generate the random variables. If $Y$ is a $U(0, 1)$ distribution, then the normal random variable x equals to $F^{-1}(Y)$. The observed variation $\sigma_{Obs}$ can be expressed in the terms of the actual process variation $\sigma_{Act}$ and NGR&R as in Eq. (14).

$$\sigma_{Obs} = \frac{\sigma_{Act}}{\sqrt{1-(NGR\&R)^2}} \qquad (14)$$

Table 6 shows six cases of monte carlo simulation. Suppose that the shear strength of the adhesive joint of slider is normally distributed with μ=149.9 gf, actual sigma σ_Act of 10 gf, LSL = 110 gf, and $Cp_{Act}$ = 1.33. For the current shear test method with NGR&R of 57.15%, the observed sigma σ_Obs equals to 12.186. Equation (13) was used to simulate the shear force obtained from the slider shear test system.

The python which is an open source software was coded to perform the monte carlo simulation so that the difference between PPM_Obs and PPM_Act will be observed. The random variable for this simulation is the shear strength under the normality assumption as in Eq. (13). The actual and observed sigma are the input for the monte carlo simulation. Total six cases with different actual $Cp$ and %NGR&R were simulated and the simulation results are shown in Table 6. The defectives in ppm for both actual and observed sigma can be estimated by running the simulation code of python. Figure 11(a) displays the defectives found from 1,000,000 units produced under the

actual $Cp$ of 1.33 and %NGR&R of 57.15% for case 1 in Table 6. For each replicate of the simulation, the 1,000,000 uniform random numbers Y were generated to simulate the shear strength and the defective units were counted as displayed in Fig. 11(a). Next, total 2,000 replicates of the simulation were run to observe the mean of $PPM_{Obs}$ and $PPM_{Act}$ depicted in Fig. 11(b) and 11(c), respectively. The over reject rate for this case is equal to 497.1 ppm which well agrees with Eq. (12). The simulation results confirm that reducing the measurement error can improve the accuracy of estimating the process capability index.

## 4. Conclusion

This paper proposes the appropriate procedure to evaluate and improve the slider shear test system of the adhesive bonding for the HGA, which is a vital component of the hard disk drive. Based on the design of new slider shear test system, the experiments, and simulation results, the major conclusions can be drawn as follows:

1. The major design improvements of the slider shear test system based on the six sigma methodology included the shear force direction, shear tool, fixture, and the measuring system. The new design concept of shear test system adopted the concept of shear test from [20] because the commercial tool is not available in the market.

2. The current method yielded inaccurate shear strength because of the incorrect failure mode after the shear test. The fabrication of the new shear tester and the assessment of measurement error were done with good results. There is no suspension flexure damage as before. The failure mode after the shear test obtained from the new slider shear test system occurred at the adhesive bond line, which is the preferable failure mode. The fixture made by the new concept works precisely and was reliably proven by actual testing with the assistance of statistical analysis.

3. The experiments were done, and the NGR&R study yielded a %NGR&R of 57.15% for the current shear test method and a %NGR&R of 9.28% for the new shear test method. Therefore, the new tester is acceptable based on the AIAG's recommendation (%NGR&R less than 10%). This means that the new shear tester can improve both the accuracy and

precision of the measurement system for the shear strength of the adhesive joint of slider.

4. The monte carlo simulation confirms that high measurement error can increase the over reject rate of the assembly process. Reducing the measurement error can improve the estimation of the process capability index and decrease the over rejection rate. The new shear test method can improve the accuracy in estimating the potential process capability index ($Cp$) by 21.28%. Consequently, the cost of quality due to misclassification can be decreased.

According to the research results, the new slider shear test system can properly be used with high confidence and reliability in the production line for statistical process control. Reduction of measurement error can enhance the effectiveness of the quality assurance system. The proposed procedures can be used as the effective framework for improving the measurement system.
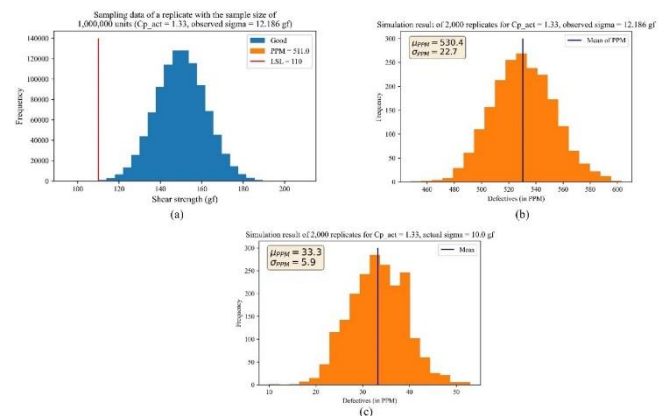


Fig. 11. (a) The sampling data from a replicate of monte carlo simulation from python for case 1; (b) The $PPM_{Obs}$ obtained from the simulation results of 2,000 replicates for case 1; (c) The $PPM_{Act}$ obtained from the simulation results of 2,000 replicates for case 1.

## Acknowledgement

Table 6. The simulation results for the $PPM_{Act}$, $PPM_{Obs}$, and over reject rate.

| Case | % NGR&R | $Cp_{Act}$ | μ | $\sigma_{Act}$ | $\sigma_{Obs}$ | $\mu_{PPM_{Act}}$ | $\mu_{PPM_{Obs}}$ | Over reject rate (ppm) |
|------|---------|-----------|-------|--------|--------|-----------|-----------|------------------------|
| 1 | 57.15% | 1.33 | 149.9 | 10 | 12.186 | 33.3 | 530.4 | 497.1 |
| 2 | 9.28% | 1.33 | 149.9 | 10 | 10.043 | 33.3 | 35.7 | 2.4 |
| 3 | 57.15% | 1.20 | 146.0 | 10 | 12.186 | 159.4 | 1568.1 | 1408.7 |
| 4 | 9.28% | 1.20 | 146.0 | 10 | 10.043 | 159.4 | 169.0 | 9.6 |
| 5 | 57.15% | 1.00 | 140.0 | 10 | 12.186 | 1350.4 | 6913.4 | 5563.0 |
| 6 | 9.28% | 1.00 | 140.0 | 10 | 10.043 | 1350.4 | 1408.5 | 58.1 |

# Appendices

Table A.1 The shear force (gf) according to the DOE plan for the current shear test system.

| Run No. | Parts | Operators | Shear force (current method) (gf) | Run No. | Parts | Operators | Shear force (current method) (gf) |
|---|---|---|---|---|---|---|---|
| 1 | 1 | 1 | 121.8 | 46 | 6 | 1 | 46.6 |
| 2 | 1 | 2 | 88.2 | 47 | 6 | 2 | 70.4 |
| 3 | 1 | 3 | 77.9 | 48 | 6 | 3 | 72.3 |
| 4 | 2 | 1 | 83.3 | 49 | 7 | 1 | 54.0 |
| 5 | 2 | 2 | 130.0 | 50 | 7 | 2 | 56.7 |
| 6 | 2 | 3 | 133.1 | 51 | 7 | 3 | 47.7 |
| 7 | 3 | 1 | 107.8 | 52 | 8 | 1 | 103.0 |
| 8 | 3 | 2 | 99.1 | 53 | 8 | 2 | 120.3 |
| 9 | 3 | 3 | 107.5 | 54 | 8 | 3 | 125.9 |
| 10 | 4 | 1 | 83.6 | 55 | 9 | 1 | 126.8 |
| 11 | 4 | 2 | 111.2 | 56 | 9 | 2 | 100.8 |
| 12 | 4 | 3 | 89.1 | 57 | 9 | 3 | 82.2 |
| 13 | 5 | 1 | 76.5 | 58 | 10 | 1 | 118.3 |
| 14 | 5 | 2 | 65.5 | 59 | 10 | 2 | 126.0 |
| 15 | 5 | 3 | 88.4 | 60 | 10 | 3 | 143.7 |
| 16 | 6 | 1 | 77.4 | 61 | 1 | 1 | 78.7 |
| 17 | 6 | 2 | 95.3 | 62 | 1 | 2 | 81.8 |
| 18 | 6 | 3 | 98.6 | 63 | 1 | 3 | 102.2 |
| 19 | 7 | 1 | 67.2 | 64 | 2 | 1 | 109.0 |
| 20 | 7 | 2 | 61.4 | 65 | 2 | 2 | 134.1 |
| 21 | 7 | 3 | 54.1 | 66 | 2 | 3 | 114.1 |
| 22 | 8 | 1 | 94.8 | 67 | 3 | 1 | 112.4 |
| 23 | 8 | 2 | 123.8 | 68 | 3 | 2 | 124.0 |
| 24 | 8 | 3 | 84.7 | 69 | 3 | 3 | 83.0 |
| 25 | 9 | 1 | 147.0 | 70 | 4 | 1 | 134.0 |
| 26 | 9 | 2 | 150.8 | 71 | 4 | 2 | 98.1 |
| 27 | 9 | 3 | 128.0 | 72 | 4 | 3 | 68.3 |
| 28 | 10 | 1 | 86.1 | 73 | 5 | 1 | 45.9 |
| 29 | 10 | 2 | 100.0 | 74 | 5 | 2 | 55.2 |
| 30 | 10 | 3 | 144.3 | 75 | 5 | 3 | 67.8 |
| 31 | 1 | 1 | 89.9 | 76 | 6 | 1 | 59.3 |
| 32 | 1 | 2 | 69.3 | 77 | 6 | 2 | 91.0 |
| 33 | 1 | 3 | 52.7 | 78 | 6 | 3 | 86.7 |
| 34 | 2 | 1 | 116.6 | 79 | 7 | 1 | 65.4 |
| 35 | 2 | 2 | 158.1 | 80 | 7 | 2 | 56.8 |
| 36 | 2 | 3 | 98.7 | 81 | 7 | 3 | 62.4 |
| 37 | 3 | 1 | 107.5 | 82 | 8 | 1 | 104.3 |
| 38 | 3 | 2 | 86.5 | 83 | 8 | 2 | 99.0 |
| 39 | 3 | 3 | 97.2 | 84 | 8 | 3 | 113.5 |
| 40 | 4 | 1 | 118.4 | 85 | 9 | 1 | 151.2 |
| 41 | 4 | 2 | 106.0 | 86 | 9 | 2 | 112.9 |
| 42 | 4 | 3 | 56.9 | 87 | 9 | 3 | 150.9 |
| 43 | 5 | 1 | 54.5 | 88 | 10 | 1 | 126.8 |
| 44 | 5 | 2 | 56.0 | 89 | 10 | 2 | 154.4 |
| 45 | 5 | 3 | 79.5 | 90 | 10 | 3 | 112.1 |

Table A.2 The shear force (gf) according to the DOE plan for the new shear test system.

| Run No. | Parts | Operators | Shear force (new method) (gf) | Run No. | Parts | Operators | Shear force (new method) (gf) |
|---|---|---|---|---|---|---|---|
| 1 | 1 | 1 | 75.5 | 46 | 6 | 1 | 78.4 |
| 2 | 1 | 2 | 78.0 | 47 | 6 | 2 | 79.0 |
| 3 | 1 | 3 | 76.8 | 48 | 6 | 3 | 75.0 |
| 4 | 2 | 1 | 119.5 | 49 | 7 | 1 | 91.0 |
| 5 | 2 | 2 | 118.4 | 50 | 7 | 2 | 91.2 |
| 6 | 2 | 3 | 123.2 | 51 | 7 | 3 | 94.8 |
| 7 | 3 | 1 | 118.4 | 52 | 8 | 1 | 111.0 |
| 8 | 3 | 2 | 121.0 | 53 | 8 | 2 | 110.8 |
| 9 | 3 | 3 | 124.3 | 54 | 8 | 3 | 114.2 |
| 10 | 4 | 1 | 83.2 | 55 | 9 | 1 | 135.2 |
| 11 | 4 | 2 | 85.4 | 56 | 9 | 2 | 129.4 |
| 12 | 4 | 3 | 86.2 | 57 | 9 | 3 | 135.2 |
| 13 | 5 | 1 | 83.2 | 58 | 10 | 1 | 131.7 |
| 14 | 5 | 2 | 80.3 | 59 | 10 | 2 | 128.0 |
| 15 | 5 | 3 | 81.2 | 60 | 10 | 3 | 129.0 |
| 16 | 6 | 1 | 80.2 | 61 | 1 | 1 | 75.5 |
| 17 | 6 | 2 | 78.6 | 62 | 1 | 2 | 70.2 |
| 18 | 6 | 3 | 78.6 | 63 | 1 | 3 | 78.6 |
| 19 | 7 | 1 | 91.0 | 64 | 2 | 1 | 118.5 |
| 20 | 7 | 2 | 93.4 | 65 | 2 | 2 | 120.6 |
| 21 | 7 | 3 | 89.9 | 66 | 2 | 3 | 122.5 |
| 22 | 8 | 1 | 111.0 | 67 | 3 | 1 | 120.3 |
| 23 | 8 | 2 | 112.0 | 68 | 3 | 2 | 118.4 |
| 24 | 8 | 3 | 113.5 | 69 | 3 | 3 | 121.8 |
| 25 | 9 | 1 | 130.4 | 70 | 4 | 1 | 82.1 |
| 26 | 9 | 2 | 132.0 | 71 | 4 | 2 | 83.2 |
| 27 | 9 | 3 | 134.2 | 72 | 4 | 3 | 79.8 |
| 28 | 10 | 1 | 129.0 | 73 | 5 | 1 | 81.2 |
| 29 | 10 | 2 | 120.4 | 74 | 5 | 2 | 81.0 |
| 30 | 10 | 3 | 130.2 | 75 | 5 | 3 | 83.4 |
| 31 | 1 | 1 | 75.6 | 76 | 6 | 1 | 78.3 |
| 32 | 1 | 2 | 70.2 | 77 | 6 | 2 | 80.7 |
| 33 | 1 | 3 | 77.2 | 78 | 6 | 3 | 78.3 |
| 34 | 2 | 1 | 120.8 | 79 | 7 | 1 | 91.5 |
| 35 | 2 | 2 | 118.5 | 80 | 7 | 2 | 88.4 |
| 36 | 2 | 3 | 119.0 | 81 | 7 | 3 | 91.7 |
| 37 | 3 | 1 | 122.0 | 82 | 8 | 1 | 111.0 |
| 38 | 3 | 2 | 121.6 | 83 | 8 | 2 | 115.4 |
| 39 | 3 | 3 | 117.6 | 84 | 8 | 3 | 112.4 |
| 40 | 4 | 1 | 84.6 | 85 | 9 | 1 | 132 |
| 41 | 4 | 2 | 83.4 | 86 | 9 | 2 | 131.4 |
| 42 | 4 | 3 | 86.4 | 87 | 9 | 3 | 130.5 |
| 43 | 5 | 1 | 83.0 | 88 | 10 | 1 | 132.2 |
| 44 | 5 | 2 | 80.8 | 89 | 10 | 2 | 128.0 |
| 45 | 5 | 3 | 81.2 | 90 | 10 | 3 | 127.3 |

# References

[1] Y. Guan, X. Chen, F. Li, and H. Gao, "Study on the curing process and shearing tests of die attachment by Ag-epoxy electrically conductive adhesive," *Int. J. Adhes. Adhes.*, vol. 30, pp. 80-88, 2010. [Online]. Available: https://doi.org/10.1016/j.ijadhadh.2009.09.003

[2] Y. Wan, S. Li, X. Hu, Y. Qiu, T. Xu, Y. Li, and X. Jiang, "Shear strength and fracture surface analysis of Sn58Bi/Cu solder joints under a wide range of strain rates," *Microelectron. Reliab.*, vol. 86, pp. 27-37, 2018. [Online]. Available: https://doi.org/10.1016/j.microrel.2018.05.007

[3] B. R. Mose, I. S. Son, and D. K. Shin, "Adhesion strength of die attach film for thin electronic package at elevated temperature," *Microelectron. Reliab.*, vol. 91, pp. 15-22, 2018. [Online]. Available: https://doi.org/10.1016/j.microrel.2018.07.143

[4] P. Jojibabu, Y. X. Zhang, A. N. Rider, J. Wang, and B. G. Prusty, "Synergetic effects of carbon nanotubes and triblock copolymer on the lap shear strength of epoxy adhesive joints," *Compos. B. Eng.*, vol. 178, pp. 107457, 2019. [Online]. Available: https://doi.org/10.1016/j.compositesb.2019.107457

[5] S. D. Vacche, S. Forzano, A. Vitale, M. Corrado, and R. Bongiovanni, "Glass lap joints with UV-cured adhesives: Use of a perfluoropolyether methacrylic resin in the presence of an acrylic silane coupling agent," *Int. J. Adhes. Adhes.*, vol. 92, pp. 16-22, 2019. [Online]. Available: https://doi.org/10.1016/j.ijadhadh.2019.04.003

[6] Ž. Unuk, A. Ivanič, V. Ž. Leskovar, M. Premrov, and S. Lubej, "Evaluation of a structural epoxy adhesive for timber-glass bonds under shear loading and different environmental conditions," *Int. J. Adhes. Adhes.*, vol. 95, p. 102425, 2019. [Online]. Available: https://doi.org/10.1016/j.ijadhadh.2019.102425

[7] Y. Tan, X. Li, G. Chen, Q. Gao, G. Q. Lu, and X. Chen, "Effects of thermal aging on long-term reliability and failure modes of nano-silver sintered lap-shear joint," *Int. J. Adhes. Adhes.*, vol. 97, p. 102488, 2020. [Online]. Available: https://doi.org/10.1016/j.ijadhadh.2019.102488

[8] L. Nele and B. Palmieri, "Electromagnetic heating for adhesive melting in CFRTP joining: Study, analysis, and testing," *Int. J. Adv. Manuf. Technol.*, vol. 106, pp. 5317–5331, 2020. [Online]. Available: https://doi.org/10.1007/s00170-019-04910-9

[9] L. D. C. Ramalho, R. D. S. G. Campilho, J. Belinha, and L. F. M. Silva, "Static strength prediction of adhesive joints: A review," *Int. J. Adhes. Adhes.*, vol. 96, p. 102451, 2020. [Online]. Available: https://doi.org/10.1016/j.ijadhadh.2019.102451

[10] R. C. Dehaghani, D. Cronin, and J. Montesano, "Performance and failure assessment of adhesively bonded non-crimp fabric carbon fiber/epoxy composite single lap joints," *Int. J. Adhes. Adhes.*, vol. 105, p. 102776, 2021. [Online]. Available: https://doi.org/10.1016/j.ijadhadh.2020.102776

[11] L. Guo, J. Liu, H., Xia, X. Li, X. Zhang, and H. Yang, "Effects of surface treatment and adhesive thickness on the shear strength of precision bonded joints," *Polym. Test.*, vol. 94, p. 107063, 2021. [Online]. Available: https://doi.org/10.1016/j.polymertesting.2021.107063

[12] H. Zhou, H. Y. Liu, H. Zhou, Y. Zhang, X. Gao, and Y. W. Mai, "On adhesive properties of nano-silica/epoxy bonded single-lap joints," *Mater. Des.*, vol. 95, pp. 212-218, 2016. [Online]. Available: https://doi.org/10.1016/j.matdes.2016.01.055

[13] *Adhesives - Determination of Tensile Lap-Shear Strength of Rigid-To-Rigid Bonded Assemblies*, ISO 4587, 2003.

[14] *Standard Test Method for Apparent Shear Strength of Single-Lap-Joint Adhesively Bonded Metal Specimens by Tension Loading (Metal-to-Metal)*, ASTM D1002 -10, 2019.

[15] *Standard Test Method for Lap Shear Adhesion for Fiber Reinforced Plastic (FRP) Bonding*, ASTM D5868 -01, 2014.

[16] J. Y. H. Chia, B. Cotterell, and T. C. Chai, "The mechanics of the solder ball shear test and the effect of shear rate," *Mater. Sci. Eng. A*, vol. 417, pp. 259-274, 2006. [Online]. Available: https://doi.org/10.1016/j.msea.2005.10.064

[17] G. Chen, L. Yu, Y. H. Mei, X. Li, X. Chen, and G. Q. Lu, "Reliability comparison between SAC305 joint and sintered nanosilver joint at high temperatures for power electronic packaging," *J. Mater. Process. Technol.*, vol. 214, pp. 1900-1908, 2014. [Online]. Available: https://doi.org/10.1016/j.jmatprotec.2014.04.007

[18] C. A. Yang, C. R. Kao, and H. Nishikawa, "Development of die attachment technology for power ic module by introducing indium into sintered nano-silver joint," in *Proceedings of the 2017 IEEE 67th Electronic Components and Technology Conference (ECTC),* pp. 1974-1980. [Online]. Available: https://doi.org/10.1109/ECTC.2017.78

[19] N. Pflügler, G. M. Reuther, M. Goroll, D. Udiljak, R. Pufall, and B. Wunderle, "Experimental determination of critical adhesion energies with the advanced button shear test," *Microelectron. Reliab.*, vol. 99, pp. 177-185, 2019. [Online]. Available: https://doi.org/10.1016/j.microrel.2019.06.001

[20] *Characterization of Interfacial Adhesion in Semiconductor Packages*, JEDEC Standard, JEP167A, 2013.

[21] P. R. Bradler, J. Fischer, R. Wan-Wendner, and R. W. Lang, "Shear test equipment for testing various polymeric materials by using standardized multipurpose specimens with minor adaptions," *Polym. Test.*, vol. 75, pp. 93-98, 2019. [Online]. Available: https://doi.org/10.1016/j.polymertesting.2019.01.024

[22] G. H. Oh, S. J. Joo, J. W. Jeong, and H. S. Kim, "Effect of plasma treatment on adhesion strength

and moisture absorption characteristics between epoxy molding compound/silicon chip (EMC/chip) interface," *Microelectron Reliab*, vol. 92, pp. 63-72, 2019. [Online]. Available: https://doi.org/10.1016/j.microrel.2018.11.004

[23] S. Yao, E. Ozturk, and D. Curtis, "Work holding assessment of an UV adhesive and fixture design method," *Int. J. Adv. Manuf. Technol.*, vol. 106, pp. 741–752, 2020. [Online]. Available: https://doi.org/10.1007/s00170-019-04635-9

[24] R. B. D. Pereira, R. S. Peruchi, A. P. Paiva, S. C. Costa, and J. R. Ferreira, "Combining Scott-Knott and GR&R methods to identify special causes of variation," *Meas.*, vol. 82, pp. 135-144, 2016. [Online]. Available: https://doi.org/10.1016/j.measurement.2015.12.033

[25] L. M. M. Araújo, R. G. N. Paiva, R. S. Peruchi, P. R. Junior, and J. H. D. F. Gomes, "New indicators for measurement error detection in GR&R studies," *Meas.*, vol. 140, pp. 557-564, 2019. [Online]. Available: https://doi.org/10.1016/j.measurement.2019.03.059

[26] F. A. D. Almeida, G. F. Gomes, R. C. Sabioni, J. H. D. F. Gomes, V. R. D. Paula, A. P. Paiva, and S. C. D. Costa, "A gage study applied in shear test to identify variation causes from a resistance spot welding measurement system," *Stroj. Vestn-J. Mech. E.*, vol. 64, no. 10, pp. 621-631, 2018. [Online]. Available: https://doi.org/10.5545/sv-jme.2018.5235

[27] G. Aquila, R. S. Peruchi, P. R. Junior, L. C. S. Rocha, A. R. D. Queiroz, E. D. O. Pamplona, and P. P. Balestrassi, "Analysis of the wind average speed in different Brazilian states using the nested GR&R measurement system," *Meas.*, vol. 115, pp. 217-222, 2018. [Online]. Available: https://doi.org/10.1016/j.measurement.2017.10.048

[28] I. S. B. Ferreira, R. S. Peruchi, N. J. Fernandes, and P. Rotella Junior, "Measurement system analysis in angle of repose of fertilizers with distinct granulometries," *Meas.*, vol. 170, p. 108681, 2021. [Online]. Available: https://doi.org/10.1016/j.measurement.2020.108681

[29] K. Mittal, P. C. Tewari, and D. Khanduja, "On the fuzzy evaluation of measurement system analysis in a manufacturing and process industry environment: A comparative study," *Manag. Sci. Lett.*, vol. 8, pp. 201–216, 2018. [Online]. Available: https://doi.org/10.5267/j.msl.2018.3.001

[30] D. C. Montgomery, *Design and Analysis of Experiments*, 9th ed. Hoboken, NJ, USA: John Wiley & Sons, Inc., 2017.

[31] Automotive Industry Action Group – AIAG, *Measurement System Analysis—Reference Manual*, 4th ed. Chrysler, Ford, General Motors Supplier Quality Requirements Task Force, 2010.

[32] S. Jin, M. S. Kim, S. Kanayama, and H. Nishikawa, "Shear properties of In-Bi alloy joints with Cu substrates during thermal aging," *Microelectron Reliab*, vol. 88–90, pp. 795-800, 2018. [Online]. Available: https://doi.org/10.1016/j.microrel.2018.07.046

[33] A. Brik, M. Goddi, J. Dhahri, and N. B. Fredj, "Assessing process capability index using sampling plan in the presence of measurement system errors," *Int. J. Adv. Manuf. Technol.*, vol. 102, pp. 3301-3313, 2019. [Online]. Available: https://doi.org/10.1007/s00170-019-03404-y

[34] M. R. Maleki, A. Amiri, and P. Castagliola, "Measurement errors in statistical process monitoring: A literature review," *Comput. Ind. Eng.*, vol. 103, pp. 316-329, 2017. [Online]. Available: https://doi.org/10.1016/j.cie.2016.10.026

**Santi Pumkrachang** is a PhD candidate in the Faculty of Engineering, King Mongkut's University of Technology North Bangkok, Thailand. He has experience in the hard disk drive industry for 24 years. His experience and the area of interests include the improvement on the manufacturing and assembly process in hard disk drive assembly, process optimization, assembly process development, measurement system, tool design, fixture design, and automation process.

**Krisada Asawarungsaengkul** graduated in Production Engineering from King Mongkut's University of Technology North Bangkok and took his Master's degree from Chulalongkorn University. He received his PhD degree in Industrial Engineering from Sirindhorn International Institute of Technology, Thammasat University. Currently, he is an Associate Professor in the Faculty of Engineering at King Mongkut's University of Technology North Bangkok, Thailand. His research interests include lean six sigma, optimisation in operations and manufacturing system, improvement on the electronic assembly manufacturing, advanced quality control, and smart factory technology. He has involved in the industrial research projects. He has published several articles in refereed journals and conference proceedings.

**Parames Chutima** received his Engineering degree from Chulalongkorn University. He received his Master's degree from Chulalongkorn University and Asian Institute of Technology. He received his PhD degree in Manufacturing Engineering and Operations Management from the University of Nottingham. Currently, he is a Professor in the Faculty of Engineering at Chulalongkorn University, Bangkok, Thailand. His research interests include multi-objective optimisation in operations management, production planning and control of assembly lines, just-in-time production systems and simulation modelling. He is the author of several international publications in conference proceedings and referred journals.